Biochimica et Biophysica Acta, 731 (1983) 97–108
Elsevier

BBA 71655

NONELECTROLYTE SUBSTITUTION FOR WATER IN PHOSPHATIDYLCHOLINE BILAYERS

R.V. McDANIEL [a], T.J. McINTOSH [b,*] and S.A. SIMON [a,c]

Departments of [a] Physiology, [b] Anatomy, and [c] Anesthesiology, Duke University Medical Center, Durham, NC 27710 (U.S.A.)

(Received November 8th, 1982)
(Revised manuscript received February 18th, 1983)

Key words: Phosphatidylcholine bilayer; Interdigitated phase; Water substitution; Glycerol; Differential scanning calorimetry; X-ray diffraction; Van der Waals force

Glycerol substitutes for water in multilamellar phosphatidylcholine liposomes in that the fluid spaces between bilayers, as well as their main transition temperatures, heat capacities, and ethalpies are very similar in water and in pure glycerol. One major difference is that the gel state phase of dipalmitoylphosphatidylcholine (DPPC) in glycerol consists of bilayers with fully interdigitated hydrocarbon chains. Interdigitated DPPC phases are also formed in ethylene glycol or in methanol (at low methanol content). In solutions of glycerol and water, the fluid spacing between bilayers is a function of mole fraction of glycerol X_g, reaching maximum values at $X_g \cong 0.1$ for lipid in the liquid crystalline phase and at $X_g \cong 0.3$ for the gel phase. These changes are explained in terms of a modification of the long-range Van der Waals attractive forces by glycerol.

Introduction

Since water and phospholipids constitute two of the major components of biological membranes, it is of inherent interest to understand how the interaction of these components affects bilayer structure, thermal behavior, and forces between bilayers. Previous investigators [1,2] approached this problem by systematically removing water from lipids. We have taken a different approach, substituting glycerol, ethylene glycol, or methanol (either partially or completely) for water. The glycerol/water/phosphatidylcholine system was studied in greatest detail. Glycerol is used as a cryoprotectent [3,4] and has been shown to substitute for water in several biological systems [5,6]. More recently, glycerol and ethylene glycol have been used as fusogens [7].

We find that multilamellar liposomes can be formed in pure glycerol and ethylene glycol. Under these conditions egg phosphatidylcholine liposomes have the same fluid space that they would have in water. However, in solutions of glycerol and water, the fluid spacing between bilayers is a function of the mole fraction of glycerol in the added solution (X_g), being maximum at $X_g \cong 0.1$ for egg phosphatidylcholine and at $X_g \cong 0.3$ for gel state DPPC bilayers. These maxima are explained in terms of glycerol changing the dielectric permittivity of the fluid space, thereby modifying the long-range Van der Waals attractive forces between bilayers. Also, at low water content, glycerol, ethylene glycol and methanol cause the gel phase acyl chains of DPPC to fully interpenetrate the hydrocarbon chains of the apposing monolayer. Similar interdigitated gel phases have previously been found in certain soaps [8] and in phosphatidylglycerol [9]. We find that the transition from the interdigitated phase (L_{β_I}) to the liquid-crystalline phase (L_α) occurs at the same temperature and enthalpy (within 1 degree C and 2 kcal/mol) as in water.

* To whom correspondence should be addressed.

Materials

Glycerol (Aldrich, gold label grade, over 99.55% pure), ethylene glycol and methanol (Fischer) were used as obtained. Water was deionized and then doubly distilled. DL-α-Dipalmitoylphosphatidylcholine (DL-DPPC), L-α-dipalmitoylphosphatidylcholine (L-DPPC or DPPC), and egg phosphatidylcholine (egg PC) were used as obtained from Sigma and/or Avanti Polar Lipids.

Methods

Calorimetry. Differential scanning calorimetry (DSC) was performed in a heat conduction calorimeter based on the design of Suurkuusk et al. [10]. Lipid powder, glycerol, and water were sequentially weighed into 0.5 ml stainless steel, vapor-tight DSC sample chambers. The water content of the lipid powder was ascertained by measuring the transition temperature of the powder and using the DPPC-water phase diagram [1] (Fig. 10A). Water content of the glycerol solutions was measured by refractive index using an Abbé refractometer. The apparent specific heat of glycerol/water was calculated to change linearly with weight fraction from 0.575 cal/g per degree in pure glycerol to 1.0 cal/g per degree in pure water [5]. The apparent molar heat capacity, C_p, of DPPC was determined by calorimetry as previously described [11]. The calorimeter voltage from the thermopiles was corrected for the calorimeter time constant, heating rate, sensitivity, and sample chamber heat capacity to obtain the total heat capacity of the glycerol/water/lipid mixture. The calculated glycerol/water mixture heat capacity was then subtracted to give the lipid C_p. The enthalpy of transition (ΔH_m) was obtained from the integrated area of the heat flow vs. temperature curves by converting the temperature axis to a time axis from a knowledge of the heating rate. For DPPC/glycerol/water experiments the total heat of fusion (ΔH_f) is expressed as $\Delta H_f = \Delta H_m + (0.3 \pm 0.1)$ kcal/mol, where the second smaller term represents the single phase heat capacity contribution to the enthalpy of melting [11]. The reported mole fractions of glycerol (X_g) are those of the added solution phase and include all water bound to the lipid. Samples were heated for 2 to 16 h above the lipid transition temperature before calorimetric data were obtained. Repeated scans at 0, 4, 60, and 99 wt% glycerol showed superimposable cooling and heating curves. The heating rates were varied from 2.5 to 34 degrees C/h to test for metastable transition states. Samples examined using thin-layer chromatography after completion of the DSC scans gave single spots.

X-ray diffraction. Samples were prepared by adding known compositions of non-electrolytes to lipid powder, heating them in an oven above T_m for several hours under nitrogen in a small glass vial, and then vortexing the sample while still above T_m. Sufficient solution was added to lipid to form a visible excess phase. Samples were drawn into quartz capillaries by negative pressure and sealed. Exposures and data analysis were performed as previously described [12].

Results

Scanning calorimetry

Fig. 1 shows the effect of glycerol on the phase transitions of L-DPPC · trihydrate from 40 to 80°C for values of 0, 10, 20, 39, 65 wt% of glycerol in lipid with no added water. No transitions are observed between 18 and 40°C. L-DPPC · trihydrate exhibits a single broad endothermic peak with a maximum at 68°C. Upon addition of 10 wt% glycerol (1 mole glycerol per mole DPPC · trihydrate) two small melting peaks appear at 41–42°C in addition to the transition at 68°C. At 20 wt% glycerol, four transitions are detected – a sharp one at 42°C, a low temperature shoulder at 41°C, and two broad transitions at 49°C and 68°C. As up to 65 wt% glycerol is added (16 moles glycerol per mole DPPC) the 49°C and 68°C peaks both disappear. Under these conditions, the enthalpy of the 42°C peak increases to its maximum value of 9 kcal/mol (at 7 moles glycerol per mole of lipid). The inset of Fig. 1 shows the total heat absorbed (ΔH_T) from 20°C to 45°C. ΔH_T reaches its maximum at a 7 : 1 mole ratio of glycerol to lipid. The excess glycerol phase, as determined by X-ray diffraction, also occurs at 7 : 1 glycerol/lipid mole ratio (Fig 5).

Heating curves for L-DPPC and DL-DPPC in excess water and in water/glycerol solutions are shown in Figs. 2A–2C. Fig. 2A shows a heat

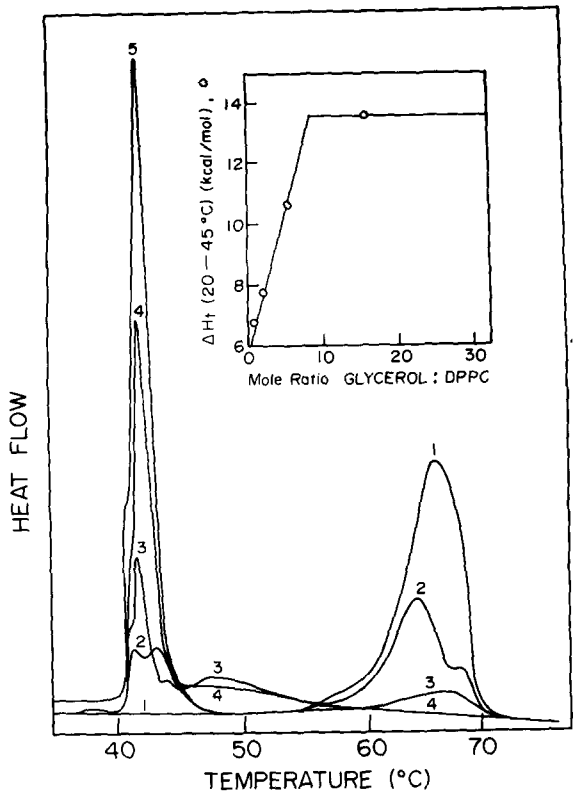

Fig. 1. Glycerination of L-α-dipalmitoylphosphatidylcholine·trihydrate. Heat flow (ordinate) vs. temperature (abscissa) curves obtained from scanning calorimetry at a 21 degrees C/h heating rate. Samples consisted of 72.35 mg of L-DPPC·trihydrate (curve 1) with the addition of 8.10 mg (curve 2), 16.45 mg (curve 3), 46.20 mg (curve 4), and 133.70 mg (curve 5) of 99.55 wt% glycerol. (Inset) Calorimetric evidence for the occurrence of an excess glycerol phase (G) at 7 to 9 moles glycerol per mole of lipid. Open circles are the total heats absorbed on heating from 20°C to 45°C from the data of the main figure using $C_p = 0.2$ kcal/mol per degree C for all single phases.

capacity (C_p) vs. temperature curve for L-DPPC in excess water. It is known that the calorimetric behavior of DL-DPPC is the same as that of L-DPPC in excess water [13]. The transition temperature, T_m, and enthalpy (ΔH_m) for the pre- and main-transitions are 35°C, 41°C and 1.5 kcal/mol, 8.6 kcal/mol, respectively. The maximum value of the heat capacity (C_p^{max}) is 21 kcal/mol per degree C, and the width at half height for the main transition is 0.4 degree C. These results agree with previous studies [14]. The heat capacity C_p in the $L_{\beta'}$, $P_{\beta'}$ and L_α phases is 200 ± 50 cal/mol per degree C [12]. C_p^{gel} and C_p^{lc} are not significantly altered by glycerol, $X_g = 0.94$. Fig. 2B shows a series of L-DPPC heat flow vs. time curves from $0.13 \leq X_g \leq 0.83$. Fig. 2C shows similar curves for DL-DPPC. Several small changes in transition temperature (T_m) occur as a function of glycerol concentration. Complete substitution of glycerol for water does not alter T_m by more than 1 degree C. Increasing the glycerol concentration to $X_g = 0.5$ first decreases and then eliminates the pretransition peak (Fig. 2B upper curves). T_m for the broadened main transition is raised by about 0.5°C with high temperature shoulders appearing at $0.3 < X_g < 0.4$. For $0.5 < X_g < 0.94$, the main transition can be resolved into two smaller transitions, one at 41.3 ± 0.2°C (denoted T1) and the other at 42.2 ± 0.3°C (denoted T2). T2 occurs at a slightly higher temperature (42.4 ± 0.2°C) in DL-DPPC than in L-DPPC (42.2 ± 0.3°C). T1 is resolvable as a separate peak in DL-DPPC and as a prominent shoulder in L-DPPC (compare Figs. 2B and 2C). Scanning one peak requires at least 15 calorimeter time constants at 2.3 degrees C/h scan rate. This assures a good approximation to thermal equilibrium during the phase transition.

Fig. 3 shows the dependence of ΔH_m for both L-DPPC and DL-DPPC on X_g. Gel phases present at the various values of X_g, as determined by X-ray diffraction (see below), are listed at the top of the figure. Between $X_g = 0.50$ and $X_g = 0.72$, the enthalpy of T1 decreases linearly while the enthalpy of T2 increases linearly with X_g. Between $X_g = 0.72$ and $X_g = 0.94$, ΔH_m approaches the value it has in excess water. ΔH_m for the T1 + T2 transitions increases linearly with glycerol content from the control value of 8.6 kcal/mol to 11.4 kcal/mol at $X_g = 0.72$, whereupon it decreases to a value approaching that of the lipid in excess water as X_g approaches 1.0.

X-ray diffraction

At 20°C the diffraction patterns for all DPPC specimens with glycerol concentrations from $X_g = 0$ to $X_g = 0.97$, consist of several lamellar low-angle reflections and one or two wide-angle bands. For all diffraction patterns, the sharp lamellar reflections extend to $R \cong 0.08$ Å^{-1} in reciprocal space (about 13 Å resolution). The repeat period for DPPC in excess water is 64 Å. As the glycerol

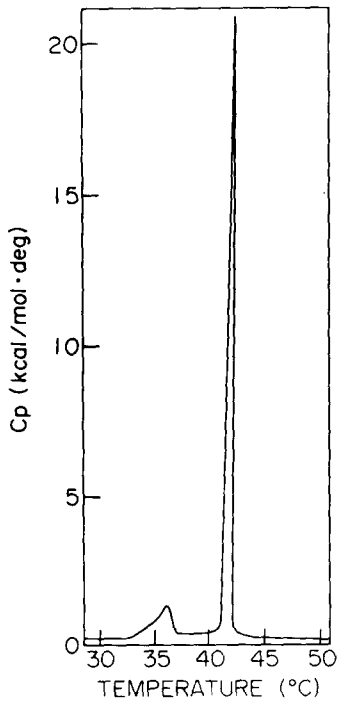

A

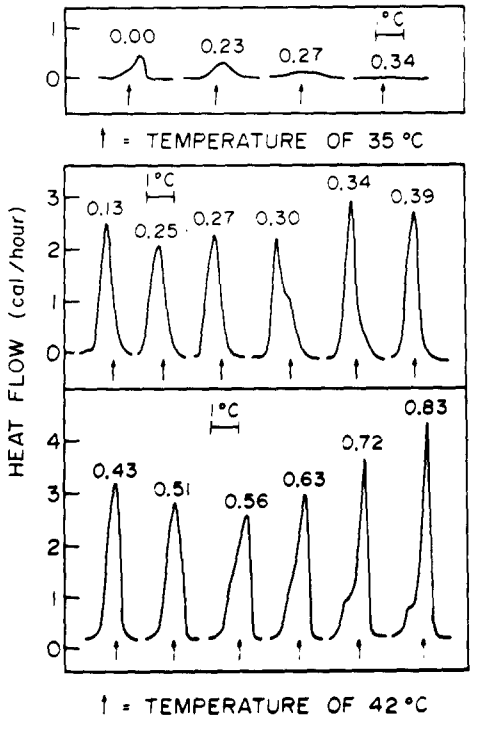

B

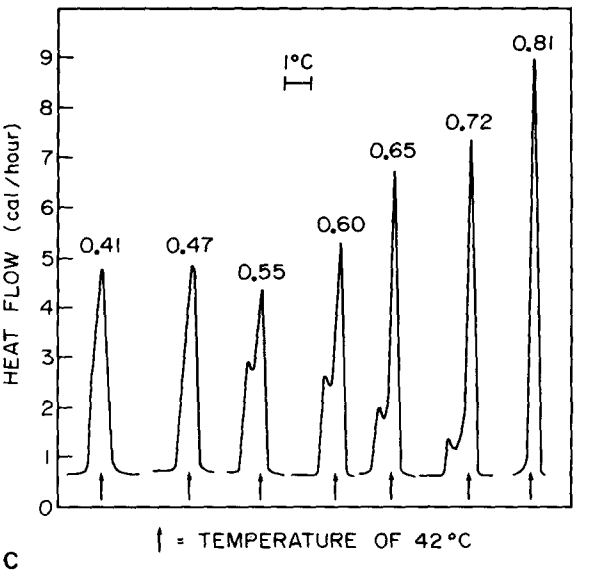

C

Fig. 2. Hydration of glycerinated L-DPPC and DL-DPPC. Lipid concentrations in the sample are < 35 wt%. Heating rate is 2.3 degrees C per h. (A) Heat capacity (ordinate) vs. temperature (abcissa) curve for L-DPPC in water. (B) Heat flow (ordinate) vs. temperature (abcissa) curves for L-DPPC in glycerol/water solutions. Mole fractions of glycerol in the added solutions (X_g) are: 0.13, 0.25, 0.27, 0.30, 0.34, 0.39, 0.43, 0.51, 0.56, 0.63, 0.72, and 0.83 as denoted on the figure. Upper curves show pretransition region for X_g values of: 0.00, 0.23, 0.27, and 0.34. All higher X_g values showed no pretransition. (C) Heat flow (ordinate) vs. temperature (abcissa) curves for DL-DPPC in glycerol/water mixtures. Mole fractions (X_g) of glycerol in the added aqueous solutions are: 0.41, 0.47, 0.55, 0.60, 0.65, 0.72, and 0.81 as denoted on the figure. No pretransitions were observed.

concentration is increased from $X_g = 0$ to $X_g \leq 0.3$, the repeat increases to 72 Å (see Fig. 4). For $X_g \geq 0.3$, the repeat period decreases and reaches its minimum value of 48 Å at $X_g = 0.97$. For $0 \leq X_g \leq 0.4$, the wide-angle pattern consists of a sharp reflection at 4.20 Å and a broad band centered at 4.11 Å. This pattern indicates a 'quasi-hexagonal' packing of tilted lipid chains [15]. At $X_g \cong 0.44$, the wide-angle pattern contains two sharp bands at 4.18 Å and 4.12 Å. For $X_g \geq 0.53$, the wide-angle pattern consists of a single sharp reflection at about 4.10 Å indicating a hexagonal packing of untilted lipid chains [15].

To obtain additional information on the structure of the DPPC/glycerol multilayers, that is, $X_g = 0.97$, we determined the repeat period and structure amplitudes as a function of the lipid/

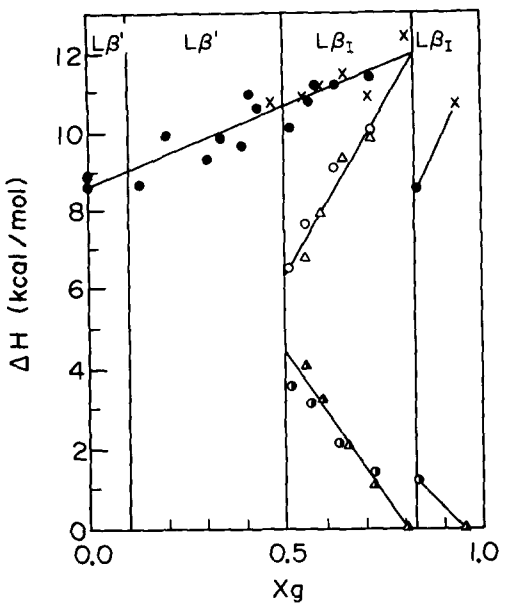

Fig. 3. Enthalpy of transition for L-DPPC and DL-DPPC in glycerol/water solutions as a function of glycerol mole fraction (X_g) in the solutions. Dots (L-DPPC) and crosses (DL-DPPC) are total values of ΔH_m. Lower points are ΔH_m values for $t_m(T1) = 41.3 \pm 0.2°C$. Open circles (L-DPPC) and triangles (DL-DPPC) are ΔH_m values for $t_m(T2) = 42.2 \pm 0.3°C$. Lipid phases for each range of X_g are noted on the figure.

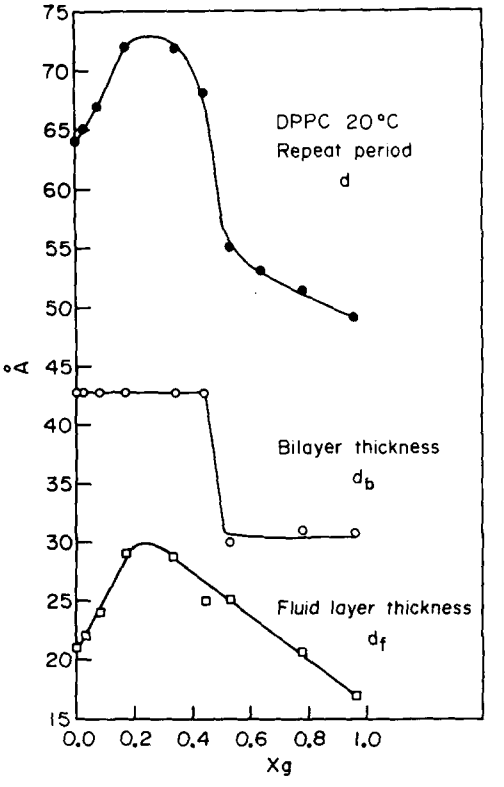

Fig. 4. X-ray parameters for DPPC as a function of mole fraction of glycerol (X_g). The solid circles (●) represent the repeat periods d and the open circles (○) and open squares (□) represent the bilayer widths and fluid layer thicknesses, respectively, as determined from electron density profiles (see Fig. 7).

glycerol weight ratio. At 20°C, the repeat period for DPPC ranges from 40 Å (at 71% DPPC/29% glycerol) to 50 Å (at 55% DPPC/45% glycerol), with the repeat period remaining between 48 Å and 50 Å at higher glycerol concentrations (see Fig. 5). In Fig. 6, the structure amplitudes for these DPPC/glycerol experiments are plotted versus the reciprocal space coordinate R (solid circles). All of the data points fall on a smooth curve with two nodes in the range $0.02 < R < 0.08$, indicating that the structure of the bilayer remains constant as more glycerol ($X_g = 0.97$) is added to the lipid, and that the increase in repeat period from 40–50 Å represents swelling of the fluid space between bilayers [16]. Also included in Fig. 6 are structure factors of DPPC in excess glycerol/water solutions with $X_g = 0.53$ (crosses) and $X_g = 0.79$ (open circles). The electron densities of these solutions (which correspond to 85% and 95% glycerol by weight, respectively) are close enough to the electron density of glycerol that these data points also fall on the smooth curve. Electron density profiles can be calculated if the phase angle for each reflection is determined. Since the bilayers are centrosymmetric, each phase angle must be 0 or π. However, the swelling curve limits the number of phase choices, as all structure factors on the same node must have the same phase angle. Since the center of the hydrocarbon region of the bilayer must have a lower electron density than the glycerol fluid space, the first node must have a phase angle of π. The shape of the transform strongly suggests that there is a change of phase at $R \cong 0.048$ Å^{-1}. Moreover, we have calculated electron density profiles for each of the data sets assuming both possible phase combinations (π, 0) and (π, π) for the two nodes. Only for the (π, 0) combination does the bilayer region of the profile remain constant for each swelling experiment. Thus, (π, 0) is the correct phase combination for the two nodes of

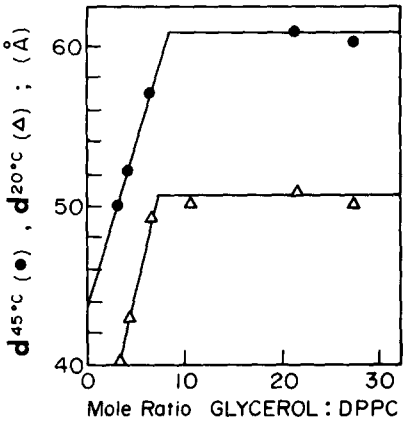

Fig. 5. X-ray repeat periods for DPPC at 20°C and 45°C as a function of mole ratio of glycerol ($X_g = 0.97$) to DPPC with no added water.

Fig. 6 and is the phase combination for DPPC in $X_g = 0.53$, $X_g = 0.79$, and $X_g = 0.97$. The phase combination for DPPC in water has previously been determined [15], and the same phase choice was used for DPPC in glycerol/water solutions for $0 \leq X_g < 0.5$, since the intensity distributions were similar for diffraction patterns from all of these samples. Fig. 7 shows electron density profiles for DPPC in excess solution, for $X_g = 0$, 0.16, 0.44, 0.53, and 0.96. In each profile, the two high-density peaks represent the lipid headgroups, and the central low-density regions between the headgroup peaks represent the bilayer hydrocarbon core. At the outside of each profile, the narrow, medium density regions correspond to the fluid spaces between bilayers. The major difference in the profiles for $X_g = 0.0$, 0.16, and 0.44 is that the electron density of the fluid layer increases with increasing glycerol concentration. For the profiles in Fig. 7, the fluid space is largest for $X_g = 0.16$, and smallest for $X_g = 0.96$. The width of the bilayer is constant at $d_b \cong 43$ Å for $0 \leq X_g \leq 0.44$, but decreases abruptly by 13 Å for $X_g \geq 0.53$. The bilayer width, d_b, as measured by the peak-to-peak separations in the electron density profiles, and fluid width (d_f), are plotted in Fig. 4. The sudden drop in bilayer thickness at $X_g \cong 0.5$ correlates with the change in wide-angle diffraction pattern from the double sharp 4.18 Å and 4.12 Å reflections observed at $X_g = 0.44$, to the single sharp 4.10 Å reflection observed for $X_g \geq 0.5$. For $X_g \leq 0.44$, the lipid is in the $L_{\beta'}$ phase in which there is a deep trough in the geometric

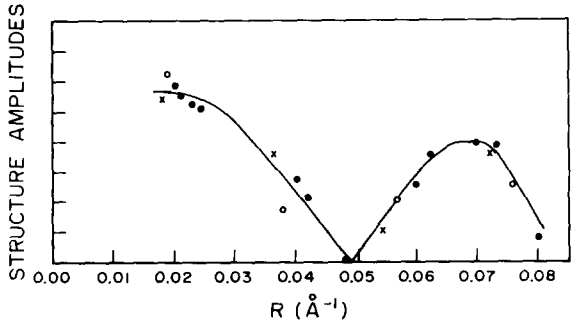

Fig. 6. Structure amplitudes for a series of swelling experiments with DPPC in glycerol, $X_g = 0.97$ (solid circles). Also included are structure factors for DPPC in excess glycerol/water solutions, $X_g = 0.53$ (crosses) and $X_g = 0.79$ (open circles).

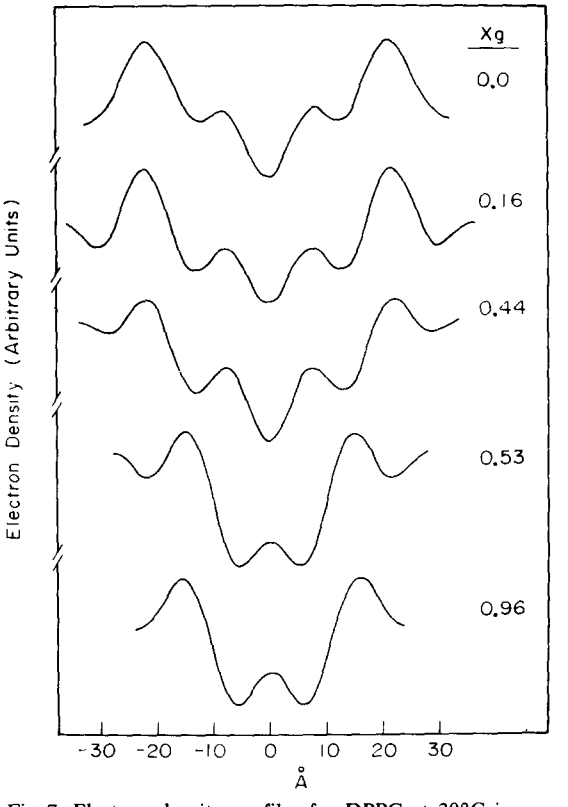

Fig. 7. Electron density profiles for DPPC at 20°C in excess aqueous solutions containing various mole fractions of glycerol (X_g) in the aqueous phase.

center of the bilayer corresponding to the localization of the low-density terminal methyl groups (Fig. 7, profiles for $X_g = 0$, 0.16, and 0.44). In the profiles for $X_g = 0.53$ and 0.96, there are two density throughs, separated by about 12 Å in the hydrocarbon region of the bilayer, suggesting that the lipid hydrocarbon chains from opposing monolayers have interpenetrated. This same type of interdigitation of lipid hydrocarbon chains has been observed by Vincent and Skoulios [8] for potassium stearate, by Ranck et al. [9] for dipalmitoylphosphatidylglycerol (DPPG) and by McIntosh et al. [17] for fully hydrated DPPC containing certain amphiphilic small molecules. Our data (Figs. 6 and 7) for DPPC in glycerol are consistent with the swelling curves and electron density profiles for DPPG by Ranck et al. [9]. Also, following Ranck et al. [17], we calculate the partial lipid thickness (d_l) and the average surface area (S) available to one lipid molecule by the equations

$$d_l = d\left(1 + \frac{\bar{v}_g}{\bar{v}} \cdot \frac{1-c}{c}\right)^{-1} \quad (1)$$

and

$$S = 2(M\bar{v}/d_l N_A)\cdot 10^{-24} \text{ (in Å}^2\text{)}$$

where $\bar{v}_g$ and $\bar{v}$ are the partial specific volumes of glycerol and DPPC, c is the weight of the lipid divided by the weight of the sample, M is the molecular weight of DPPC, and N_A is Avagadro's number. The results of these calculations from the data of Fig. 5 are shown in Table I. Also included are the values for the cross sectional area per hydrocarbon chain (Σ) which was calculated [13] using the wide angle spacing s ($\Sigma = 2s^2/(3)^{1/2}$).

TABLE I

X-RAY PARAMETERS FOR ANHYDROUS DPPC/GLYCEROL MULTILAYERS

% Glycerol	d (Å)	d_l (Å)	S (Å^2)	Σ (Å^2)	S/Σ
29	40.2	29.9	78.0	19.2	4.06
35	43.3	29.8	78.3	19.2	4.08
44	48.9	29.5	79.3	19.4	4.09

As shown in the last column of Table I, the ratio of the area per lipid molecule and area per hydrocarbon chain is approx. 4, additional evidence that the lipid hydrocarbon chains are interdigitated for $X_g \geq 0.53$. A value of 2 would be predicted for a non-interdigitated bilayer phase. Note that the values of partial lipid thickness (d_l) as calculated from Eqn. 1 are in close agreement with the bilayer width (d_b) as measured from electron density profiles (Fig. 4).

Fig. 8 shows electron density profiles for DPPC in ethylene glycol and in methanol. These profiles are similar to that of DPPC in glycerol ($X_g = 0.96$), except for the densities of the fluid layers between bilayers. In the case of methanol, the electron density between bilayers is even lower than in the hydrocarbon region of the bilayer, since the density of methanol is less than the density of gel state lipid hydrocarbon chains.

Data for liquid crystalline phase lipids in glycerol are shown for DPPC at 45°C in Fig. 5 and for egg PC at 20°C in Fig. 9. In the case of DPPC (Fig. 5) the repeat period increases 10 Å as the lipid goes from the gel at 20°C to the liquid-crystalline phase at 45°C. The 10 Å repeat period increase upon heating at 30% to 45% glycerol, with

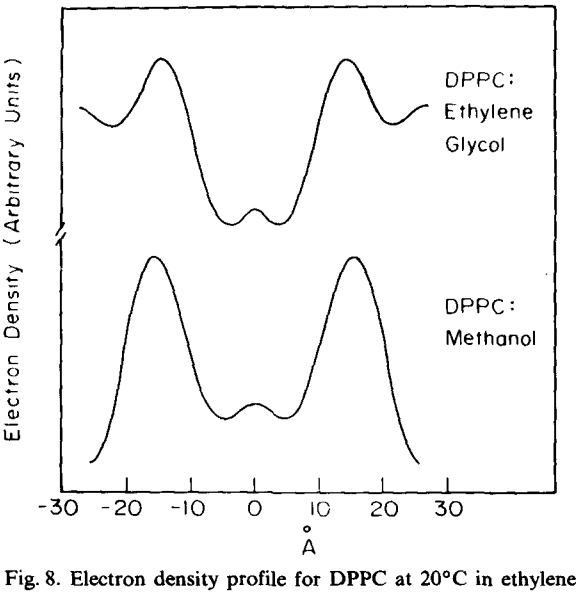

Fig. 8. Electron density profile for DPPC at 20°C in ethylene glycol (61 wt% DPPC/39 wt% ethylene glycol) and methanol (66 wt% DPPC/34 wt% methanol) with no added water.

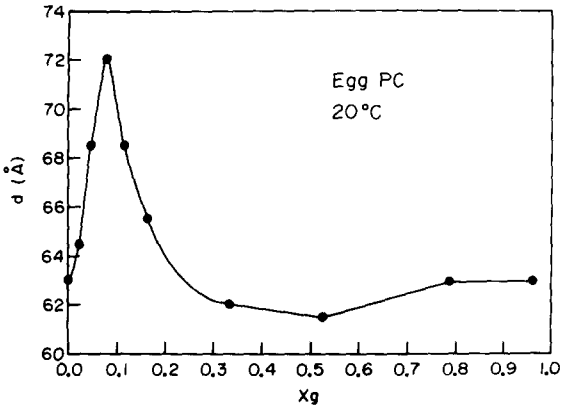

Fig. 9. Repeat period d for egg phosphatidylcholine as a function of mole fraction of glycerol (X_g).

no excess glycerol present, shows that the bilayer thickness increases upon melting. At 45°C, the values of d_1 and S for DPPC are 36.9 ± 1.3 Å and 71.7 ± 2.4 Å^2, respectively. These numbers are very similar to values reported by Lis et al. [18] for DPPC bilayers in excess water at 50°C.

For egg PC in excess water/glycerol solutions the repeat period reaches a maximum at $X_g = 0.08$, whereupon it returns to its control value at $X_g = 0.33$ (Fig. 9). At higher X_g there is no significant change in d to $X_g = 0.96$.

Discussion

The interaction of selected nonelectrolytes, methanol, ethylene glycol, and glycerol, with phospholipids in the presence of various amounts of water has been studied in this paper. We have emphasized the glycerol/water/phosphatidylcholine system for two reasons. First, it is different to maintain the purity of ethylene glycol (especially when heated) as many breakdown products, such as formaldehyde, are formed [5]. Second, only very concentrated lipid dispersions can be used in methanol, since in pure methanol, phosphatidylcholines either dissolve or form micelles. Phosphatidylcholine is much more soluble in methanol than in the other nonelectrolytes, because of the lower free energy of transfer of hydrocarbon chains into methanol.

Effects of nonelectrolytes on bilayer thermodynamics and structure

Several calorimetric and X-ray results for DPPC/glycerol/water dispersions are summarized in Table II. A striking feature of the comparison between DPPC in excess water and 96 wt% glycerol is that DPPC has essentially the same thermodynamic values for the main endothermic transition (i.e., the same T_m, ΔH_m, C_p^{gel}, and C_p^{lc}) despite differences in the packing of the lipids in the gel phase under both conditions. In excess water the chains are fully extended and tilted with respect to the plane of the bilayer ($L_{\beta'}$), whereas in excess glycerol the acyl chains are interdigitated and are perpendicular to the plane of the membrane (L_{β_1}).

The fact that T_m and ΔH_m remain constant upon interdigitation can be rationalized as follows. The acyl chains for phosphatidylcholines, under fully hydrated conditions, determine the main transition characteristics [19]. The contributions of

TABLE II

PROPERTIES OF L-α-DPPC IN EXCESS WATER-GLYCEROL MIXTURES

wt% glycerol:	0	5	60	85	90	96
X_g	0	0.01	0.23	0.53	0.65	0.82
t_m (°C)	41.3	41.7	41.6	41.3	41.3	42.1
				42.1	42.1	–
ΔH_m(kcal/mol)	8.6	8.7	9.9	4.0	1.4	9.0
				7.0	10.0	–
C_p^{max}(kcal/mol/degree)	21.0	16.0	10.0	5.5	2.5	–
				9.0	14.0	16.0
$C_p^{gel,lc}$(kcal/mol/degree)	0.20	0.20	0.20	0.20	0.20	0.20
t_{pre} (°C)	36	36	36	–	–	–
Phase at 20°C	$L_{\beta'}$	$L_{\beta'}$	$L_{\beta'}$	L_{β_1}	L_{β_1}	L_{β_1}

the headgroups to the transition parameters must be small, since in the $L_{\beta'}$ phase there are twice as many headgroups per unit area as in the L_{β_1} phase. In the liquid-crystalline (L_α) phase, d, d_1, area per molecule, and C_p are virtually the same in excess glycerol and in excess water, suggesting that the chemical potential (and apparent enthalpy) of the lipids in the L_α phase under both conditions is the same. In both the $L_{\beta'}$ and L_{β_1} phases the methylene groups are in similar environments. In glycerol and in water the methylene groups are surrounded by other methylene groups but the terminal methyl groups, which are located near the geometric center of the bilayer in water, are located in the interfacial region in glycerol.

The major calorimetric difference between water and glycerol phases is that the pretransition peak is absent in the presence of glycerol in the L_{β_1} phase. This is expected since the pretransition peak is observed for lipids with chain tilt [15, 20–22], which glycerol removes.

We postulate that for the L_{β_1} phase to be induced at least two criteria must be met. Water must be removed from a particular location(s) at the interface and this displaced water must be replaced by a larger, surface active, amphiphilic solvent molecule that tends to increase the lipid interfacial area (see also the accompanying paper, Ref. 17). From the data of Tardieu et al. [15], it is known that the interdigitated phase in DPPC (at 20°C) is not induced by simply removing water. Nor is the ability to form the L_{β_1} phase correlated to the solvent's hydrogen bonding ability, since glycerol can form more hydrogen bonds than water, but methanol can form fewer hydrogen bonds than water [23]. Fig. 4 shows that the induction of the L_{β_1} phase occurs over a narrow concentration range centered at $X_g \cong 0.5$. This concentration corresponds to a volume fraction of glycerol in the bulk solution of about 0.8. Using the Gibbs absorption equation [24] it can be calculated from surface tension data [25] that at $X_g = 0.5$, 92% of the area at an air-water interface will be occupied by glycerol. Thus, when $X_g > 0.5$ only a few water molecules will be left in the interfacial region. It must be the removal of one (or more) of these waters from a particular location(s) that allows the formation of L_{β_1}. An interdigitated gel phase also forms in excess ethylene glycol and methanol (12 moles methanol per mole DPPC) for the same reasons outlined above.

Increasing the molecular area by adsorption of a larger surface active molecule would tend to increase the free energy of the $L_{\beta'}$ phase by exposing additional hydrocarbon to water as well as reducing the Van der Waals interaction between the acyl chains. Under these conditions the lower energy phase becomes the L_{β_1}. Ranck and Tocanne [26] demonstrated the L_{β_1} phase in dipalmitoylphosphatidylglycerol (DPPG) bilayers by adding choline or acetylcholine ions. They suggested that this phase is induced in DPPG when the area per

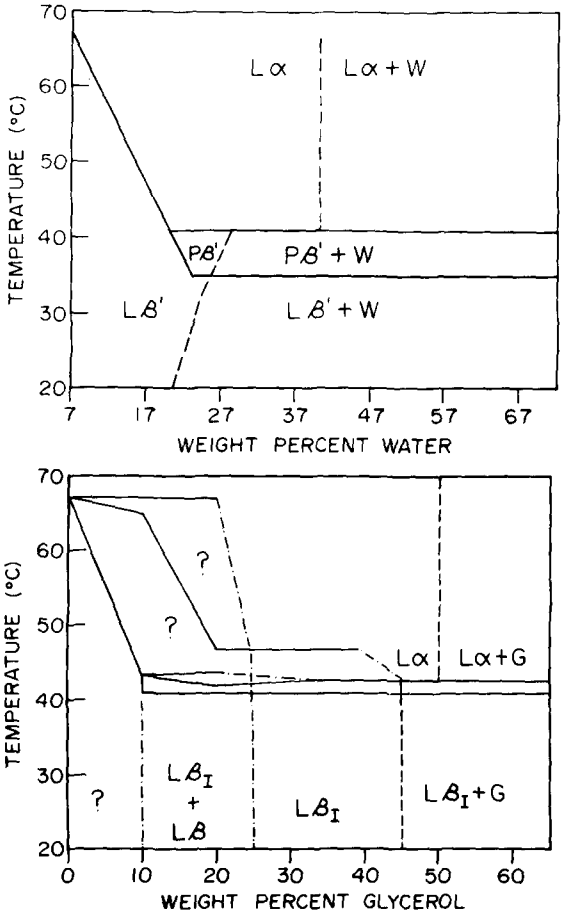

Fig. 10 (A) Phase diagram for DPPC·trihydrate and water as adapted from Chapman et al. [1] and Janiak et al. [22]. (B) Phase diagram for DPPC·trihydrate and glycerol as derived from the calorimetric and X-ray diffraction data of Figs. 1, 2, 5, and 7. G refers to an excess glycerol phase.

polar headgroup is increased. It is evident from our data that the presence of a formal charge is not necessary for the formation of the L_{β_I} phase.

Phase diagrams of DPPC · $3H_2O$/water (from Refs. 1 and 22), and DPPC · H_2O/glycerol (obtained from the data in Figs. 1, 2, 5, and 7) are shown in Figs. 10A and 10B. The vertical dashed lines represent the minimum amounts of water or glycerol needed to form an excess fluid phase, horizontal lines represent the peak heat flow temperatures obtained from the heating curves of Fig. 2, and the dotted and dashed lines represent approximate boundaries for the existence of phases to the left of these lines. The solid lines which connect various peak temperatures were constructed by interpolation of the data. Question marks represent regions of uncertainty as to the phase. Data was not obtained in the region below 10 wt% glycerol. The phase diagram for L-DPPC in glycerol (Fig. 10B) differs from that of L-DPPC in water (Fig. 10A) in several respects. First, not all of the lipid is converted to the glycerinated form with a continuous drop of T_m as in water. Rather, a glycerinated phase and a DPPC · trihydrate phase coexist even when the sample is thoroughly mechanically mixed. Second, the L_{β_I} phase replaces the $L_{\beta'}$ and $P_{\beta'}$ gel phases. Third, approximately the same volume of glycerol will form an excess phase in both gel and liquid crystalline lipids, while more water will be incorporated in the liquid crystalline than in the gel phase. The liquid crystalline phase incorporates the same fluid volume in water and in glycerol. Fourth, at 10–40 wt% glycerol, several additional phase transitions occur which are not found in water. The origins of these multiple transitions were not investigated.

The phase diagram shows an excess glycerol phase in the gel at 7 moles of glycerol per mole of DPPC. The molar volume of glycerol is 120 Å^3, giving 840 Å^3 of space for glycerol for each lipid molecule. From Hauser et al. [27], the distance from the phosphate group to the carbonyl group on the longer chain is 7 Å. The fluid spacing is 15 Å and the area per two acyl chains is 38 Å^2, allowing room for 2.2 glycerol molecules

$$\left|\frac{(266\ \text{Å}^3)}{(120\ \text{Å}^3)}\right|$$

in the polar region and 4.8 glycerol molecules

$$\left|\frac{(570\ \text{Å}^3)}{(120\ \text{Å}^3)}\right|$$

in the fluid space. This accounts for the 7 glycerol molecules per DPPC molecule.

The calorimetric behavior of DPPC in dilute aqueous solutions of glycerol or ethylene glycol is markedly different from that in methanol [28,29]. Whereas glycerol and ethylene glycol [30] virtually do not change the transition parameters, increased concentrations of methanol decrease the transition temperature [31]. The freezing-point depression of the DPPC transition by methanol has been attributed to the different partition coefficients of methanol in the gel and liquid-crystalline phases [28]. Although the partition coefficients of glycerol and ethylene glycol are greater above than below T_m [32], it is obvious that the freezing-point depression analysis is not applicable to these nonelectrolytes, since T_m is not lowered by either of them. The calorimetric differences between methanol and glycerol and ethylene glycol might be related to their location in the bilayer. Methanol can dissolve in the acyl chain region, whereas glycerol and ethylene glycol are more likely to be confined to the interfacial region [32] where they substitute for water. Their ability to substitute for water may also explain why we do not observe the expected decrease in T_m that results from a lowering of the surface tension at the bilayer-fluid interface.

When both water and glycerol are present in the interface, the total enthalpy of transition is greater by 1–3 kcal/mol than when only glycerol or only water is in the interface. The formation of an uncompensated hydrogen bond in the gel phase would be consistent with this enthalpy change [33,34]. The increase in ΔH_m when ethylene glycol or glycerol is substituted for water can be rationalized in the same manner, although other explanations are possible. When $0.5 < X_g < 1.0$, two distinct main endothermic peaks occur upon transition from the L_{β_I} to L_α phases (Fig. 3, Table II). The occurrence of two peaks may be interpreted in two ways: (1) Two molecular arrangements coexist within the L_{β_I} phase with conversion from one arrangement to the other occurring in proportion to the amount of water at the interface. In this

case the two L_{β_1} phases must have the same repeat period. (2) The L_{β_1} phase could be homogeneous, but could convert to an intermediate phase between the two peaks. The enthalpy of this intermediate phase would increase in proportion to the water concentration. Presently, we cannot distinguish between these two possibilities. The possibility of metastable states was minimized by scanning very slowly.

Van der Waals forces between bilayers

The fluid spacing (d_f) between egg phosphatidylcholine bilayers is determined by the balance between an attractive long-range Van der Waals force (F_v) and a repulsive hydration force (F_r) [35]. It has been found for egg phosphatidylcholine in water [35] that these forces per unit area can be written

$$F_r = F_0 e^{-d_f/\lambda} \tag{2}$$

and

$$F_v = -\frac{1}{6\pi}\left[\tfrac{3}{2}kT{\sum_p}'\left(\frac{\epsilon_f(i\xi_p)-\epsilon_m(i\xi_p)}{\epsilon_f(i\xi_p)+\epsilon_m(i\xi_p)}\right)^2\right] \times\left(\frac{1}{d_f^3}-\frac{2}{d^3}+\frac{1}{(d+d_f)^3}\right) \tag{3}$$

where k is the Boltzmann constant, ϵ_m and ϵ_f are the dielectric permittivities of the membrane and fluid phase, respectively, and are both functions of frequency, along the imaginary frequency axis ($i\xi$) [35,36]. The prime over the summation symbol indicates that the term in $p = 0$ is taken with a factor 1/2. The term in square brackets is commonly called the Hamaker constant, $\mathcal{H}$ [36]. In the visible region of the spectrum ϵ is equal to n^2, where n is the index of refraction. Parsegian, Rand and colleagues [35] have found experimentally that λ is about 2.6 Å in water, and several authors have noted that λ corresponds to the diameter of a solvent molecule [35,37–38]. Since ϵ_f is a function of glycerol concentration, F_v should depend on X_g in the fluid phase. Moreover, if λ does depend on the molecular diameter of the molecules in the fluid phase, F_r should also depend on X_g since the diameter of glycerol is about twice that of water.

We have, in fact, found that the repeat period of egg phosphatidylcholine does depend on X_g (Fig. 9). For $0 < X_g < 0.33$, d increases and then decreases with increasing X_g. The maximum d spacing occurs at $X_g \cong 0.1$, which corresponds to an index of refraction of $n_f \cong 1.37$ at the sodium D line. This is the same index of refraction where LeNeveu et al. [35] found a maximum repeat period for egg phosphatidylcholine in sucrose and glucose solutions. LeNeveu et al. [35] attributed this phenomenon to a minimization of the term $(\epsilon_m - \epsilon_f)^2$ in the Van der Waals force, which indeed seems correct.

For $0.33 < X_g < 0.97$, the repeat period of egg phosphatidylcholine is approximately constant (Fig. 9), despite the substantial changes at all frequencies in ϵ_f and perhaps λ over this concentration range. A possible reason for this behavior is that F_r becomes much larger than F_v as d_f decreases below the equilibrium spacing in water [35]. Of particular interest is the fact that d is approximately the same for egg phosphatidylcholine in water ($X_g = 0$) and in glycerol ($X_g \cong 0.97$). Since theoretical calculations show that $\mathcal{H}$ (and hence F_v) is lower in glycerol than in water [39], this means that F_r must also be smaller in glycerol than in water. Moreover, since glycerol has been used as a fusogen, we agree with Boni et al. [40] that dehydration, by itself, is not a sufficient condition for membrane fusion. For gel state DPPC a maximum fluid spacing occurs at $X_g \cong 0.3$, corresponding to $n_f \cong 1.40$ (Fig. 4). This is 0.03 units greater than $n_f = 1.37$, where the maximum d spacing occurs in liquid crystalline state egg phosphatidylcholine (Fig. 9). This shift arises since the dielectric permittivity, ϵ_m, is greater for crystalline chains than liquid chains. In the visible frequency range, the measured index of refraction of the membrane (n_m) is higher by 0.03 or 0.04 absorbance units in the gel state than in the liquid-crystalline state. For DPPC, $n_m = 1.485$ (by extrapolating the data of Yi and MacDonald [41] to 20°C), whereas $n_m = 1.445$ for egg phosphatidylcholine [42] or $n_m = 1.454$ for egg lecithin perpendicular to the optic axis of the bilayer [43]. Therefore, although there is the expected shift in the value of X_g for the maximum d spacing for gel and liquid crystalline lipid (Figs. 4 and 9), the maximum d spacings for both gel and liquid crystalline states do not occur where $\epsilon_m = \epsilon_f$ in the optical frequency range. This discrepancy could be

due to other frequency contributions to F_v, especially the zero frequency contribution which accounts for over half the Van der Waals force [36]. In addition, it might be inadequate to characterize the membrane with a single dielectric permittivity [35].

The induction of the interdigitated phase does not change the fluid spacing between bilayers (see the profiles in Fig. 7 for $X_g = 0.44$ and $X_g = 0.53$). Neither F_v nor F_r would be expected to change appreciably by interdigitation, since F_v depends primarily on d_f rather than on d [35], and since F_r is not correlated with the surface density of the polar groups [18].

Acknowledgments

We wish to thank Mrs. S. Webb and T. Carrington for their excellent help in editing and typing this paper. This work was supported in part by Training Grant GM 07046-05 and Research Grant GM 27278.

References

1 Chapman, D., Williams, R.M. and Ladbrooke, B.D. (1967) Chem. Phys. Lipids 1, 445–475
2 Parsegian, V.A., Fuller, N. and Rand, R.P. (1979) Proc. Natl. Acad. Sci. U.S.A. 76, 2750–2754
3 Taylor, R.J., Adams, G.D.J., Boardman, C.F.B. and Wallis, R.G. (1974) Cryobiology 11, 430–438
4 Mazur, P., Miller, R.H. and Leibo, S.P. (1974) J. Membrane Biol. 15, 137–138
5 Newman, A.A. (1968) in Glycerol (Newman, A.A., ed.), p. 91, CRC Press, Cleveland
6 Schobert, B. (1979) J. Naturforsch. 34c, 699–703
7 Ahkong, Q.F., Fisher, D., Tampion, W. and Lucy, J.A. (1975) Nature 253, 194–196
8 Vincent, J.M. and Skoulios, A. (1966) Acta Cryst. 20, 432–441
9 Ranck, J.L., Keira, T. and Luzzati, V. (1977) Biochim. Biophys. Acta 488, 432–441
10 Suurkuusk, J., Lentz, B.R., Barenholtz, Y., Biltonen, R.L. and Thompson, T.E. (1976) Biochemistry 15, 1393–1401
11 McDaniel, R.V., Simon, S.A., McIntosh, T.J. and Borovyagin, V. (1982) Biochemistry 21, 4116–4126
12 McIntosh, T.J., Simon, S.A. and MacDonald, R.C. (1980) Biochim. Biophys. Acta 597, 445–463
13 Arnett, E.M. and Gold, J.M. (1982) J. Am. Chem. Soc. 104, 636–639
14 Lentz, B.R., Friere, E. and Biltonen, R.L. (1978) Biochemistry 17, 4475–4480
15 Tardieu, A., Luzzati, V. and Reman, F.C. (1972) J. Mol. Biol. 75, 711–733
16 Moody, M.F. (1963) Science 142, 1173–1174
17 McIntosh, T.J., McDaniel, R.V. and Simon, S.A. (1983) Biochim. Biophys. Acta 731, 109–114
18 Lis, L.J., McAlister, M., Fuller, N., Rand, R.P. and Parsegian, V.A. (1982) Biophys. J. 37, 657–666
19 Nagle, J.F. and Wilkinson, D.A. (1978) Biophys. J. 23, 159–175
20 Janiak, M.J., Small, D.M. and Shipley, G.G. (1976) Biochemistry 15, 4475–4580
21 McIntosh, T.J. (1980) Biophys. J. 29, 237–245
22 Janiak, M.J., Small, D.M. and Shipley, G.G. (1979) J. Biol. Chem. 254, 6068–6078
23 Stein, W.D. (1967) The Movement of Molecules Across Cell Membranes, pp. 75–81, Academic Press, New York
24 Adam, N.K. (1968) The Physics and Chemistry of Surfaces, p. 107, Dover Publications, New York
25 Handbook of Chemistry and Physics (Weast, R.C., ed.) (1974) CRC Press, Cleveland
26 Ranck, J.L. and Tocanne, J.F. (1982) FEBS Lett. 143, 171–174
27 Hauser, H., Pascher, I., Pearson, R.H. and Sundell, S. (1981) Biochim. Biophys. Acta 650, 21–51
28 Lee, A.G. (1979) Biochim. Biophys. Acta 472, 285–344
29 Jain, M.K. and Wu, N.M. (1977) J. Membrane Biol. 34, 157–207
30 Klopftenstein, W.E., De Kruijff, B., Verkleij, A.J., Demel, R.A. and Van Deenen, L.L.M. (1974) Chem. Phys. Lipids 13, 215–222
31 Hill, M.W. (1974) Biochim. Biophys. Acta 356, 117–124
32 Katz, Y. and Diamond, J. (1974) J. Membrane Biol. 17, 87–100
33 Scatchard, G., Kavanagh, G.M. and Ticknor, L.B. (1952) J. Am. Chem. Soc. 74, 3715–3724
34 Pimental, G.C. and McClellan, A.L. (1960) The Hydrogen Bond p. 221, Freeman, San Francisco
35 LeNeveu, D.M., Rand, R.P., Parsegian, V.A. and Gingell, D. (1977) Biophys. J. 18, 209–230
36 Mahanty, J. and Ninham, B.W. (1976) in Dispersion Forces, ch. 3, Academic Press, New York
37 Marcelja, S. and Radic, N. (1976) Chem. Phys. Lett. 42, 129–130
38 Christenson, H.K., Horn, R.G. and Israelachvili, J.N. (1982) J. Colloid Int. Sci. 88, 79–88
39 Brooks, D.E., Levine, Y.K., Requena, J. and Haydon, D.A. (1975) Proc. R. Soc. Lond. A. 347, 179–194
40 Boni, L.T., Stewart, T.P., Alderfer, J.L. and Hui, S.W. (1981) J. Membrane Biol. 62, 65–70
41 Yi, P.N. and MacDonald, R.C. (1973) Chem. Phys. Lipids 11, 114–134
42 Cherry, R.J. and Chapman, D. (1967) J. Mol. Biol. 30, 551–553
43 Cherry, R.J. and Chapman, D. (1969) J. Mol. Biol. 40, 19–32